

Preliminary earthquake focal mechanism forecasts for the Amatrice sequence (Central Italy)

PAMELA ROSELLI & MARIA TERESA MARIUCCI

Istituto Nazionale di Geofisica e Vulcanologia, Roma (Italy)

pamela.roselli@ingv.it

Abstract

We compare the moment tensor solutions data of the last Amatrice seismic sequence with the corresponding forecasts computed with independent information for the same territory derived from both focal mechanism catalogue and the present-day stress data (latest release). The knowledge of expected focal mechanism at the site is important to reduce the uncertainty of the Ground Motion Prediction Equation models used. For this purpose, we apply a procedure to compute, for each spatial cell, the probability to observe in the future a Normal, Reverse, and Strike-Slip event, the average distribution of the P, T, B axes and the related SHmax, for each of these types of earthquake.

I. INTRODUCTION

The seismic sequence of Amatrice (Central Italy) is characterized by a main-shock Mw 6.0 at a shallow depth of 8 km (ISIDE, <http://iside.rm.ingv.it/>), that struck the epicentral area at 1:36 a.m. (UTC) of August 24th 2016, about 10 km southeast of the town of Norcia in the Umbria region (Fig. 1). The main-shock has been followed by about 1500 aftershocks Ml 0.7 - 4.8 over the next 48 hours (ISIDe, 2016: <http://iside.rm.ingv.it/>) including a Mw 5.4 at 2:33 a.m. (UTC). The epicentral area consists of old historic towns and many small ancient villages densely populated. Including tourists and residents, nearly 300 people died although the two main shocks can be considered belonging to “moderate” earthquake magnitude class. The geological and

structural setting of the Apennines is due to the complex geodynamics mainly related to the continental collision between Africa and Eurasia plates combined with smaller intervening microplates. In this convergence conditions (started in the Early Tertiary), the lithosphere subduction beneath the Alps (to the north), Dinarides (to the east) and Apennines (to the west) has been established [e.g. Malinverno and Ryan 1986; Faccenna et al. 2001]. Nowadays stress indicators (such as borehole breakouts, earthquake focal mechanisms and active faults) point out that the axial part of the Apennine belt is characterized by a general extension about NE oriented [Lavecchia et al., 1994; Montone and Mariucci, 2016]. The epicentral area of Amatrice seismic sequence is located in the central sector of Apennines characterized by several NW-oriented fault systems (among the others Norcia, Mt. Vettore

and Laga Mts. in Figure 1) showing remarkably well exposed scarps associated

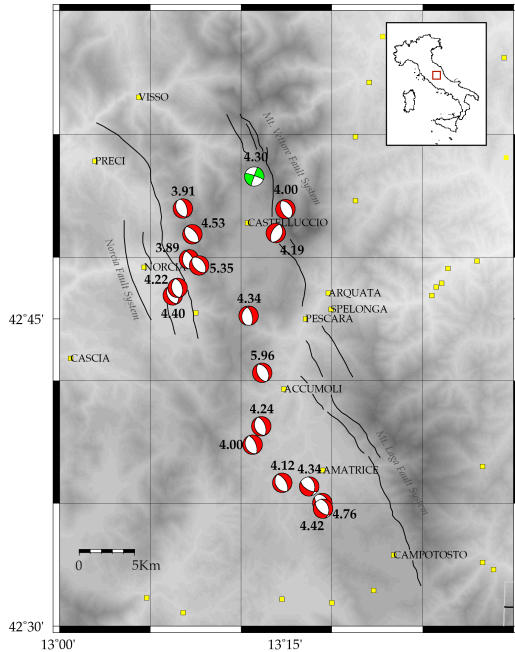


Figure 1: Location map of the study area in which are represented the focal mechanism data with $M_w \geq 3.9$ related to the Amatrice seismic sequence, red and green colours represent normal and strike-slip faulting regime, respectively; the numbers close to the beach-balls are related to the M_w values associated [Scognamiglio et al., 2016]. The black lines are the main fault systems [Centamore et al., 1992; Pierantoni et al., 2013]. Yellow squares indicate some municipalities.

with the recent activity responsible for the moderate to strong seismicity [Tondi and Cello, 2003]. It is well known that an earthquake on a fault segment may increase the state of stress on neighbour fault segments promoting the occurrence of other major shocks [Gupta and Scholz, 2000, and references therein]. Slip data from these fault structures [Cello et al., 1997] show that roughly N–S trending left-lateral strike-slip and transtensional/normal (from NNW–SSE to WNW–ESE trending) faults are all kinematically consistent with the existence of a Late Quaternary remote stress field characterized by a NE–SW-oriented min-

imum horizontal stress (σ_3 /or maximum extension) and by a NW–SE trending maximum horizontal stress (σ_1 /or maximum compression). The presence of a moderate historical seismic activity in the epicentral area is well documented in the last version of Parametric Catalogue of Italian Earthquakes [<http://emidius.mi.ingv.it/CPTI15-DBMI15/>] as Norcia 1979 (M_w 5.8), Umbria-Marche Apennines 1997 (M_w 5.6 and 6.0), L’Aquila 2009 (M_w 6.3) among the others. The seismic hazard connected to this area has been well constrained according to the last Italian Seismic Hazard Map MPS04 [MPS Working Group 2004]; the magnitude value of 24th August main-shock is within the magnitude limits of moderate-strong earthquakes occurred in the past in this region. The Ground Motion Prediction Equations (GMPEs) are useful to obtain information about the expected PGA values in a given site and hundreds of them are present in literature and applied in different region in the world [Douglas, 2011]. The use of GMPEs represents a source of uncertainty in the Probabilistic Seismic Hazard Analysis (PSHA). The reduction of this epistemic uncertainty is also linked to the expected focal mechanism type associated to the next large earthquake at the given site [Convertito and Herrero, 2004; Strasser et al., 2006; Roselli et al., 2016]. Thus, GMPEs would become more accurate if the expected style of faulting is known. In this regard, we apply a procedure to compute (for each spatial cell) the probability to observe in the future a normal (NF), reverse (RF), and strike-slip (SS) faulting event, and the average distribution of the P, T and B axes for each of these types of earthquake [Roselli et al., submitted]. In this paper, we present an application to the Amatrice epicentral area of the procedures proposed and applied by Roselli et al. [submitted] to obtain the focal mechanism forecasts, the derived maximum horizontal stress (SHmax) for whole Italian territory and to compare them with the main shocks of the sequence.

II. DATA

The study area is between 13° - 13.50° E and 42.50° - 43° N, where we select and process the focal plane parameters related to 93 earthquakes ($M_w \geq 4$) occurred from 1908 and 2015 mainly derived from the European RCMT catalogue (<http://www.bo.ingv.it/RCMT/searchRCMT.html>) and used in the stress map [Montone and Mariucci, 2016; Table S2a]. After performing a careful classification based on the interval range of P, T and B stress axes plunges following Zoback [1992], we assign the stress regime to 93 earthquakes with 71 NF, 16 RF and 6 SS events in order to compute the expected focal mechanisms parameters (forecasts). We compare these forecasts with the 17 focal mechanism parameter data ($M_w \geq 3.9$) of the recent Amatrice seismic sequence (until 30th September) achieved by Scognamiglio et al. [2016]. By using the same data selection criteria previously used, they are classified as 16 NF and 1 SS.

III. METHODOLOGY APPLIED

We implement the computation of the focal mechanism forecasts by using the *Total Weighted Moment Tensor* (TWMT) method [Roselli et al., 2015; Roselli et al., submitted] that has been applied to forecast the focal mechanisms for the next large earthquake in Italy. This application is mostly rooted on the assumption that the focal mechanism of earthquakes in the same (small) region remains the same through time [Kagan, 1992, 2000] and the tectonic stress field components are assumed to be constant in time for each region. The TWMT is inspired by the *Cumulative Moment Tensor* technique proposed by Kostrov [1974], subsequently exploited by Selva and Marzocchi [2004]. We apply the TWMT procedure for each spatial cell ($0.1^{\circ} \times 0.1^{\circ}$ spaced) in which we compute the probability to observe in the future a NF, RF, and SS event and the average distribution of the P, T and B axes for

each of earthquake focal mechanism categories. In particular, we apply equation (1) to calculate the average moment tensor for each possible focal mechanism $\alpha = \{NF, RF, SS\}$ where NF, RF and SS mean normal, reverse and strike-slip faulting, respectively. In other words, we average only the tectonically homogeneous information defining the *Total Weighted Moment Tensor* ($TWMT_k^{(\alpha)}$)

$$TWMT_k^{(\alpha)} = \tilde{M}_k^{(\alpha)} = \frac{\sum_{l=1}^{N_k^{(\alpha)}} M_l^{(\alpha)} \cdot \omega_{lk}}{\sum_{l=1}^{N_k^{(\alpha)}} \omega_{lk}} \quad (1)$$

where $\omega_{lk} = \frac{1}{\Delta_{lk}^2}$ is the weight dependent by the inverse of squared distance of the l -th earthquake, $N_k^{(\alpha)}$ is the number of past earthquakes at a distance $\Delta_{lk} \leq R$ from the k -th each cell. The diagonalization of $TWMT_k^{(\alpha)}$ allows us to estimate the average $T_k^{(\alpha)}, P_k^{(\alpha)}, B_k^{(\alpha)}$ for the k -th cell. In details, we estimate the seismic moment tensor parameters collecting past-data located at a maximum distance of 50 km from the centre of each cell. Then, we sum and mediate the contributions by weighing them according to inverse of squared distances. From the diagonalization of the mean moment tensor matrix obtained, we extract the P, T and B axes. Moreover, following the Zoback [1992] criteria, we assign a stress regime and then the weighted azimuths of SHmax, for each cell. The last step of our analysis is to assess the conditional probability of the focal mechanism type (for each cell) that satisfies the Kolmogorov axioms [Kolmogorov, 1956] and can be interpreted in the Bayesian perspective of bet quotient. For details see Roselli et al. [2015], Roselli et al. [submitted].

IV. AMATRICE CASE STUDY

The aim of this study is to compare the Time Domain Moment Tensors (TDMTs) computed during the Amatrice seismic sequence [Scognamiglio et al., 2016] with the forecasts obtained by the TWMT method. In Figure 2, we show the forecast focal mechanisms NF and SS types calculated for each cell (the respective seismic moment tensors, are shown in Table 1 and 2) in red and green, respectively. The yellow beach-balls represent the TDMTs of Ama-

trice sequence with $M_w \geq 3.9$ (see Figure 1). The pie charts located at the centre of the cells are representative of the conditional probability that a NF (light-red) or SS (light-green) large earthquake occurs within each one of 25 cells. In this case, the most events occurred reveal a NF mechanism according to the percentages expressed by the pie charts (about 90% NF, 10 % SS); only one event is characterized by a SS mechanism despite the very low probability associated to the forecast.

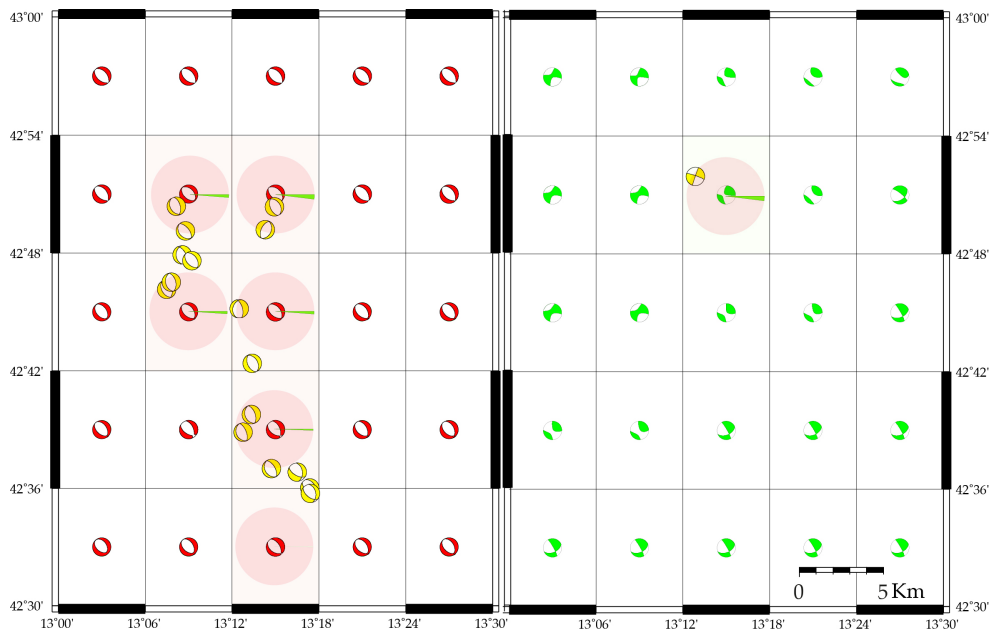


Figure 2: Location map of Amatrice seismic sequence focal mechanisms (yellow beach-balls). The forecast beach balls are prevalently NF (red) and prevalently SS (green) in the left and right panel, respectively. The cells with the pie charts are used for the comparison. The slices of pie charts in the centre of cells show the percentage associated to normal (red slices) and strike-slip (green slices) expected stress regime that is mainly NF with a SS percentage in the range 0 - 10 % (or less than 10%).

We observe a general fitting between observed and forecast data in terms of axis orientations of both NF and SS fault plane solutions. In Figure 3, we plot the forecast SHmax azimuths (black bars) compared with the observed NF (red bars) or SS (green bar) focal mechanisms. In Table 3 are shown the related orientations of

the forecast SHmax. We note a prevalent accordance between the NW-SE oriented SHmax forecasts and almost the whole real data orientations. However, the SHmax of some earthquakes seems to follow a different trend, more N-S and NNE-SSW (the yellow dashed bars in Figure 3). Finally, we show the SHmax N171

and N164 obtained from the borehole area [Mariucci et al., 2010].
breakouts in the only two wells present in that

Table 1: Seismic moment tensors obtained for each of 25 cells in Figure 2, for Normal Faulting focal mechanism type.

Lon (°)	Lat (°)	Depth (Km)	mrr	mtt	mff	mrt	mrf	mtf
13.05	42.55	10.469	-0.8112	0.3464	0.4647	-0.1905	-0.0943	-0.3938
13.05	42.65	10.293	-0.8087	0.3380	0.4707	-0.1336	-0.0750	-0.4141
13.05	42.75	10.751	-0.7912	0.3060	0.4852	-0.0680	-0.0743	-0.3747
13.05	42.85	10.586	-0.7773	0.3476	0.4297	-0.1726	0.0175	-0.4117
13.05	42.95	10.047	-0.8321	0.4124	0.4198	-0.0795	-0.0002	-0.4336
13.15	42.55	10.565	-0.8317	0.3371	0.4945	-0.1389	-0.1310	-0.4263
13.15	42.65	10.213	-0.7774	0.2997	0.4777	-0.2428	-0.1558	-0.5110
13.15	42.75	9.990	-0.8181	0.3671	0.4510	-0.1246	-0.0425	-0.4180
13.15	42.85	9.752	-0.8295	0.4079	0.4217	-0.1021	0.0159	-0.4073
13.15	42.95	10.011	-0.8271	0.3952	0.4320	-0.0656	-0.0100	-0.4285
13.25	42.55	10.363	-0.8415	0.4045	0.4371	-0.0167	-0.2626	-0.4656
13.25	42.65	10.284	-0.7964	0.3037	0.4927	-0.1572	-0.2189	-0.4776
13.25	42.75	9.626	-0.8320	0.3920	0.4400	-0.1467	-0.0312	-0.4355
13.25	42.85	8.997	-0.8535	0.4587	0.3948	-0.1207	0.0482	-0.4277
13.25	42.95	9.840	-0.8319	0.4026	0.4293	-0.0613	-0.0064	-0.4303
13.35	42.55	11.251	-0.8875	0.3784	0.5090	-0.1224	-0.1121	-0.4569
13.35	42.65	10.558	-0.8299	0.3177	0.5122	-0.1124	-0.1727	-0.4410
13.35	42.75	10.084	-0.8304	0.3562	0.4742	-0.1373	-0.0649	-0.4309
13.35	42.85	9.836	-0.8338	0.4009	0.4329	-0.0926	-0.0262	-0.4352
13.35	42.95	9.866	-0.8344	0.4101	0.4244	-0.0648	-0.0105	-0.4363
13.45	42.55	11.315	-0.8689	0.3165	0.5524	-0.1477	-0.0942	-0.4368
13.45	42.65	10.780	-0.8437	0.3063	0.5374	-0.1375	-0.1070	-0.4312
13.45	42.75	10.342	-0.8356	0.3244	0.5112	-0.1320	-0.0669	-0.4264
13.45	42.85	10.130	-0.8268	0.3767	0.4501	-0.1116	-0.0566	-0.4345
13.45	42.95	9.811	-0.8275	0.4115	0.4160	-0.0924	-0.0200	-0.4339

Table 2: Seismic moment obtained for each of 25 cells in Figure 2, for Strike-Slip focal mechanism type.

Lon (°)	Lat (°)	Depth (Km)	mrr	mtt	mff	mrt	mrf	mtf
13.05	42.55	18.002	-0.1710	0.6876	-0.5166	0.2196	-0.5945	-0.4626
13.05	42.65	13.851	-0.0668	0.0322	0.0347	0.0913	-0.1879	-0.6403
13.05	42.75	19.414	0.1025	-0.3917	0.2892	0.2551	0.0822	-0.7713
13.05	42.85	18.245	0.0935	-0.4145	0.3210	0.2200	0.0955	-0.7754
13.05	42.95	17.478	0.0480	-0.3493	0.3012	0.1785	0.0682	-0.7233
13.15	42.55	18.001	-0.1710	0.6876	-0.5166	0.2196	-0.5945	-0.4626
13.15	42.65	14.566	-0.0848	0.1450	-0.0603	0.1134	-0.2579	-0.6097
13.15	42.75	19.289	0.1015	-0.3941	0.2926	0.2513	0.0836	-0.7717
13.15	42.85	18.406	0.0947	-0.4114	0.3167	0.2248	0.0936	-0.7749
13.15	42.95	19.655	0.0186	-0.2128	0.1942	0.2224	0.0013	-0.6513
13.25	42.55	18.001	-0.1710	0.6876	-0.5166	0.2196	-0.5945	-0.4626
13.25	42.65	18.001	-0.1710	0.6876	-0.5166	0.2196	-0.5945	-0.4626
13.25	42.75	13.601	-0.0606	-0.0071	0.0677	0.0836	-0.1635	-0.6509
13.25	42.85	21.824	-0.0091	-0.0799	0.0891	0.2668	-0.0639	-0.5816
13.25	42.95	21.899	-0.0282	-0.0386	0.0668	0.2599	-0.0826	-0.5541
13.35	42.55	18.001	-0.1710	0.6876	-0.5166	0.2196	-0.5945	-0.4626
13.35	42.65	18.001	-0.1710	0.6876	-0.5166	0.2196	-0.5945	-0.4626
13.35	42.85	19.652	-0.1327	0.0945	0.0382	0.1517	-0.1364	-0.4410
13.35	42.95	23.889	-0.0798	0.1363	-0.0566	0.2884	-0.1662	-0.4539
13.45	42.55	18.000	-0.1710	0.6876	-0.5166	0.2196	-0.5945	-0.4626
13.45	42.65	18.002	-0.1710	0.6876	-0.5166	0.2196	-0.5945	-0.4626
13.45	42.75	18.002	-0.1710	0.6877	-0.5166	0.2196	-0.5946	-0.4626
13.45	42.85	31.001	-0.3238	0.8829	-0.5591	0.3627	-0.5195	-0.0129
13.45	42.95	23.571	-0.1987	0.3667	-0.1680	0.2246	-0.2687	-0.2932

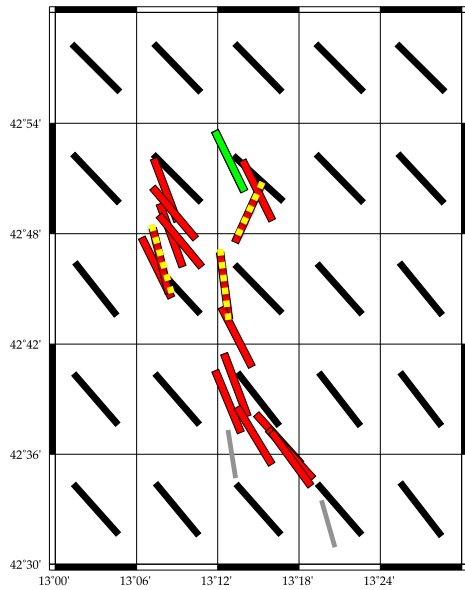


Figure 3: Location map of the forecast maximum horizontal stress (SHmax) orientations (black bars) computed for each cell; the real SHmax orientations extracted by the TDMTs are shown for NF (red and yellow dashed bars; see text for more explanations) and SS (green bar) focal mechanisms. The grey bars show the SHmax trend inferred from borehole breakouts.

Table 3: Coordinates and azimuths of SHmax inferred from the forecast moment tensor parameters, for each cell shown in Figure 3.

Lon (°)	Lat (°)	Azimuth (°)
13.05	42.55	138.314
13.05	42.65	139.169
13.05	42.75	141.874
13.05	42.85	136.509
13.05	42.95	134.988
13.15	42.55	140.412
13.15	42.65	139.076
13.15	42.75	137.335
13.15	42.85	135.060
13.15	42.95	136.060
13.25	42.55	138.541
13.25	42.65	142.054
13.25	42.75	135.778
13.25	42.85	132.425
13.25	42.95	135.740
13.35	42.55	139.119
13.35	42.65	142.215
13.35	42.75	138.411
13.35	42.85	135.744
13.35	42.95	135.307
13.45	42.55	142.361
13.45	42.65	142.515
13.45	42.75	140.823
13.45	42.85	137.084
13.45	42.95	134.817

V. DISCUSSION AND CONCLUSIONS

In this paper, we have compared the expected and observed orientation of fault plane solutions for some earthquakes of the Amatrice seismic sequence. Applying a methodology named Total Weighted Moment Tensor [Marzocchi and Selva, 2004; Roselli et al., 2015; Roselli et al., submitted], for each spatial cell ($0.1^\circ \times 0.1^\circ$), we have calculated the mean weighted moment tensor for each NF, RF and SS focal mechanism type, separately; then, we have computed the probability of occurrence associated to each of them and the related SHmax orientations (forecasts). Finally, we have compared the information extracted by real focal mechanisms of the major events occurred during the Amatrice seismic sequence (until 30th September) with these forecasts. The results show a complete agreement of the expected

and observed focal mechanism types for most earthquakes. The expected SHmax is NW-SE oriented and most observed SHmax data are aligned with this trend. Only a few earthquakes have a different NNW-SSE orientation that seems more compatible with the borehole data. This variation in the observed trend seems to suggest a possible local rotation of the stress field. Further data and investigation are needed to support this latter evidence. As the study area is located in the Central Apennines, characterized by a NE-SW oriented extension, we expected a prevalent NF focal mechanism type and a ~NW-SE trend of SHmax. Nevertheless, these observations suggest the reliability of the TWMT methodology that can be applied in more complex regions where the expected moment tensor parameters are not well defined and classified.

REFERENCES

- [Cello et al., 1997] Cello, G., Mazzoli, S., Tondi, E. and Turco, E. (1997). Active tectonics in the central Apennines and possible implications for seismic hazard analysis in peninsular Italy. *Tectonophysics*, 272(1), 43-68.
- [Centamore et al., 1992] Centamore, E., Adamoli, L., Berti, D., Bigi, G., Bigi, S., Casnedi, R., Cantalamessa, G., Fumanti, F., Morelli, C., Micarelli, A., Ridolfi, M., and Salvucci, R. (1992). Carta geologica dei bacini della Laga e del Cellino e dei rilievi carbonatici circostanti. In: *Studi Geologici Camerti*, Vol. Spec. Università degli Studi, Dipartimento di Scienze della Terra. SELCA, Firenze.
- [Convertito and Herrero, 2004] Convertito, V. and Herrero, A., (2004). Influence of Focal Mechanism in Probabilistic Seismic Hazard Analysis. *Bull. Seismol. Soc. Am.*, 94(6), 2124-2136.
- [Douglas, 2011] Douglas J. (2011). Ground-Motion Prediction Equations: 1964-2010. Final report, BRGM/RP-59356-FR.
- [Faccenna et al., 2001] Faccenna, C., Becker, T.W., Lucente, F.P., Jolivet, L. and Rossetti, F., 2001. History of subduction and back-arc extension in the Central Mediterranean. *Geophys. J. Int.*, 145(3), 809-820.
- [Gupta and Scholz, 2000] Gupta, A. and Scholz, C.H. (2000). A model of normal fault interaction based on observations and theory. *Journal of Structural Geology*, v. 22, p. 865-879.
- [ISIDe, 2016] ISIDe working group (2016) version 1.0, DOI: 10.13127/ISIDe.
- [Kagan, 1992] Kagan, Y.Y. (1992). Correlations of earthquake focal mechanisms, *Geophys. J. Int.*, 97(B4), 4823-4838.
- [Kagan, 2000] Kagan, Y.Y. (2000). Temporal correlations of earthquake focal mechanisms, *Geophys. J. Int.*, 143(3), 881-897.
- [Kolmogorov, 1956] Kolmogorov, Andrey N. *Foundations of the Theory of Probability*,

2nd English ed. Chelsea Publishing Company, New York. 1956.

[Kostrov, 1974] Kostrov, B.V. (1974). Seismic moment and energy of earthquakes, and seismic flow of rock, *Izv. Acad. Sci. USSR, Phys. Solid Earth*, 1, 23-44.

[Lavecchia et al., 1994] Lavecchia, G., Brozzetti, F., Barchi, M., Menichetti, M. and Keller, J.V.A. (1994). Seismotectonic zoning in east-central Italy deduced from an analysis of the Neogene to present deformations and related stress fields. *Geological Society of American Bulletin*, 106, 1107-1120.

[Malinverno and Ryan, 1986] Malinverno, A. and Ryan, W.B.F. (1986). Extension in the Tyrrhenian Sea and shortening in the Apennines as result of arc migration driven by sinking of the lithosphere. *Tectonics*, 5(2), 227-245.

[Mariucci et al., 2010] Mariucci, M.T., Montone, P. and Pierdominici, S. (2010). Present-day stress in the surroundings of 2009

[Montone et al., 2012] Montone, P., Mariucci, M.T. and Pierdominici, S. (2012). The Italian present-day stress map, *Geophys. J. Int.*, 189, 705-716.

[Montone and Mariucci, 2016] Montone, P. and Mariucci, M. T. (2016). The new release of the Italian contemporary stress map, *Geophys. J. Int.*, 205, 1525-1531. doi

[MPS Working Group, 2004] Mappa di Pericolosità Sismica Working Group (2004). *Redazione dell' Ordinanza PM 3274 del 20 marzo 2003. Rapporto conclusivo per il Dipartimento della Protezione Civile, INGV, Milano-Roma, April 2004, 65 pp. + 5appendices.*

[Pierantoni et al., 2013] Pierantoni, P., Deiana, G., and Galdenzi, S. (2013). Stratigraphic and structural features of the Sibillini Mountains (Umbria-Marche Apennines, Italy). *Italian Journal of Geosciences*, 132(3): 497-520.

[Roselli et al., 2015] Roselli, P., Marzocchi, Montone, P. and Mariucci, M.T. (2015).

Earthquake Focal Mechanism Forecasts and Applications in the PSHA in Italy. American Geophysical Union, Fall Meeting 2015, abstract S14B-04.

[Roselli et al., 2016] Roselli, P., Marzocchi W. and Faenza, L. (2016). Toward a new probabilistic framework to score and merge Ground-Motion Prediction Equations: the case of the Italian region, *Bull. Seismol. Soc. Am.*, 106(2), 720-733.

[Roselli et al., submitted] Roselli, P., Marzocchi, W., Mariucci, M.T. and Montone, P. (submitted). Earthquake Focal Mechanism Forecasting in Italy for PSHA purposes, Submitted to *Geoph. J. Int.*

[Scognamiglio et al., 2016] Scognamiglio L., Tinti E. and Quintiliani, M. (2016). The 2016 Amatrice seismic sequence: fast determination of time domain moment tensors and finite fault model analysis of the ML 5.4 aftershock, this issue.

[Selva and Marzocchi, 2004] Selva, J. and Marzocchi, W. (2004). Focal parameters, depth estimation, and plane selection of the worldwide shallow seismicity with $M \geq 7.0$ for the period 1900-1976, *Geochem. Geophys. Geosyst.*, 5(5), 1525-2027.

[Strasser et al., 2006] Strasser, F.O., Montaldo, V., Douglas, J. and Bommer, J.J. (2006). Comment on "Influence of Focal Mechanism in Probabilistic Seismic Hazard Analysis" by Vincenzo Convertito and Andrè Herrero, *Bull. Seismol. Soc. Am.*, 96(2), 750-753.

[Tondi and Cello, 2003] Tondi, E, and Cello, G. (2003). Spatiotemporal evolution of the Central Apennines fault system (Italy). *J. of Geodyn.*, 6 (2003) 113-128.

[Zoback, 1992] Zoback, M.L. (1992). First- and second-order patterns of stress in the lithosphere: the world stress map project, *J. Geophys. Res.*, 97(B8), 703-728.